Serotonin modulates optimized coding of natural stimuli through increased neural and behavioural responses via enhanced burst firing

Mariana M. Marquez and Maurice J. Chacron [iD]

*Department of Physiology, McGill University, Montreal, Canada*

Edited by: Ian Forsythe & Diego Contreras

Key points

- The function of serotonergic fibres onto sensory areas remains poorly understood
- We show that serotonin application enhances sensory neural and behavioural responses to second order stimuli
- Enhanced neural responses most likely occurred because of increased burst firing
- Changes in neural sensitivity due to burst firing were the best predictor of changes in behavioural sensitivity
- Our results suggest that serotonin optimizes coding of stimuli encountered during aggression.

Abstract Understanding how the processing of sensory information leads to behavioural responses remains a central problem in systems neuroscience. Here, we investigated how the neuromodulator serotonin affects neural and behavioural responses to second-order envelope stimuli within the electrosensory system of the weakly electric fish *Apteronotus leptorhynchus*. We found that serotonin application increased neuronal excitability through greater tendency for burst firing. We found that increased excitability led to overall higher neural sensitivities to higher envelope frequencies. Separating the spike train into bursts and isolated spike train components revealed that this was due to significant increases in neural sensitivity for the former but not the latter. We next investigated the consequences of such changes in sensitivity towards optimized coding of stimuli with specific statistics. Our results show that serotonin application compromised optimal coding of stimuli with statistics seen under naturalistic conditions due to changes in burst, but not isolated spike firing. Finally, we found that serotonin application increased behavioural sensitivity to envelope stimuli. Interestingly, changes in neural sensitivity due to bursts were a far better predictor of changes in behavioural sensitivity, suggesting that burst firing is decoded by downstream brain areas. Overall, our results suggest that serotonin modulates neural responses to optimize coding and perception of stimuli during behavioural contexts associated with encountering dominant conspecifics.

Mariana Marquez is a PhD student in the Physiology department at McGill University. She holds a BS in Physics from the National Autonomous University of Mexico (UNAM) in Mexico City, Mexico. During her undergraduate studies she investigated changes in the neural oscillatory patterns due to homeostatic stress. She currently works on understanding how serotonin modulates neural responses to stimuli in nature.
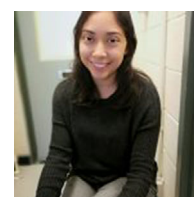
The Journal of Physiology

Corresponding author M. J. Chacron: McIntyre Medical Research Building, Room 1137, 3655 Prom. Sir William Osler, Montreal, QC, Canada, H3G 1Y6.   Email: maurice.chacron@mcgill.ca

Introduction

Organisms must efficiently process natural stimuli in order to survive and it has become clear that efficient processing must adapt to changes in the environment (Wark *et al.* 2007; Sharpee *et al.* 2014). It is thought that neuro-modulators, such as serotonin, mediate this adaption (Marder, 2012). Although the serotonergic system is highly conserved across vertebrate species (Parent, 1981), understanding its function in sensory processing has, however, been complicated. This is because serotonergic input impacts sensory processing through a variety of receptors that are most likely expressed differentially across cell types. Such differential expression mediates a variety of effects, for instance increases and decreases in neural responsiveness to specific stimuli (Hurley *et al.* 2004). In this regard, studies focusing on model organisms for which neural responses to natural stimuli associated with different behavioural contexts are well-understood are likely to make progress towards understanding the function of serotonergic neuromodulation on sensory processing.

The electrosensory system of gymnotiform weakly electric fish benefits from well-characterized neural circuitry (Bell & Maler, 2005), natural stimulus statistics (Fotowat *et al.* 2013; Metzen & Chacron, 2014) and behavioural responses (Hupe & Lewis, 2008). These fish generate an electric field surrounding their body through electric organ discharge (EOD) and sense perturbations of this field through an array of electroreceptor afferents (EAs) on their skin (Turner *et al.* 1999). EAs synapse onto pyramidal cells within the electrosensory lateral line lobe (ELL) whose responses to electrosensory stimuli have been extensively characterized (Chacron *et al.* 2011; Marsat *et al.* 2012; Krahe & Maler, 2014; Huang & Chacron, 2017; Metzen & Chacron, 2019). Natural electrosensory stimuli comprise those encountered during social interactions. Specifically, when two conspecifics are located close to one another, interference between their EODs gives rise to a sinusoidal modulation (i.e. a beat or first order) whose amplitude (i.e. the envelope or second order) increases when the distance between both animals decreases (Yu *et al.* 2012). Further studies have revealed that the spectral power of natural electrosensory envelopes decays as a power law as a function of increasing frequency (Metzen & Chacron, 2014). Interestingly, ELL pyramidal cells display high-pass tuning characteristics that oppose this decaying power, such that the resulting neural response power is independent of frequency (i.e. 'temporally whitened'), which is a signature of optimal coding as information

transmission is maximized (Rieke *et al.* 1996; Mitchell *et al.* 2018), and which ensures that behavioural sensitivity is matched to stimulus power (Huang *et al.* 2016). Temporal whitening is due to descending input (i.e. feed-back) which helps 'sculpt' the neural tuning curve in order to match natural stimulus statistics (Huang *et al.* 2018). ELL pyramidal cells also receive large amounts of neuromodulatory input (Marquez *et al.* 2013) including serotonergic fibres from the raphe nuclei (Johnston *et al.* 1990; Deemyad *et al.* 2011). While previous studies have shown that serotonergic neuromodulation affects ELL pyramidal cell responses to first order stimuli (Deemyad *et al.* 2013; Marquez & Chacron, 2018), how such input affects responses to envelopes has not been investigated to date.

Methods

Ethical approval

All experimental procedures were approved by McGill University's animal care committee under protocol 5285 and were performed according to the guidelines of the Canadian Council on Animal Care. The investigators understand the ethical principles under which *The Journal* operates and that their work complies with the animal ethics checklist. All evidence suggests that the stress levels experienced by the animals under the experimental conditions described below are no greater than those experienced under naturalistic conditions (Hitschfeld *et al.* 2009).

Origin and source of the animals

Wild-caught specimens of the weakly electric fish *Apteronotus leptorhynchus* of either sex were used in this study and were acquired from tropical fish suppliers (Importations Mirdo, Montreal, QC, Canada). Fish were acclimated to laboratory conditions in accordance with published guidelines (Hitschfeld *et al.* 2009).

Access to food and water

Animals were fed once a day.

Euthanasia

Severely sick animals were euthanized by MS-222 over-dose (Sigma-Aldrich, St-Louis, MO, USA, 1 g l^{-1}, gills)

followed by decapitation as per approved protocol 5285 and according to the guidelines of the Canadian Council on Animal Care.

Surgical procedures

Surgical procedures have been described in detail previously (Huang *et al.* 2018; Metzen *et al.* 2018). Briefly, 0.1–0.6 mg of tubocurarine (Sigma-Aldrich, St-Louis, MO, USA) was injected intramuscularly to immobilize the fish for electrophysiology and behavioural experiments. The fish was then transferred to an experimental tank (30 cm × 30 cm × 10 cm) containing water from the animal's home tank and respired by a constant flow of oxygenated water through its mouth at a flow rate of ~ 10 ml min^{-1}. Subsequently, the animal's head was locally anaesthetized by liberally applying lidocaine ointment (5%; AstraZeneca, Mississauga, ON, Canada), the skull was then partly exposed, and a small window was opened over the ELL recording site. It is important to note that previous studies have shown that weakly electric fish under these conditions display electrical behaviours that are identical to those observed in both restrained and freely moving animals (Hitschfeld *et al.* 2009). At the end of the experiment, animals were euthanized by MS-222 overdose (Sigma-Aldrich, 1 g l^{-1}, gills) followed by decapitation as per approved protocol 5285 and according to the guidelines of the Canadian Council on Animal Care.

Pharmacology

Glutamate (1 mM; Sigma-Aldrich) and serotonin (1 mM; Sigma-Aldrich) were dissolved in saline (111 mM NaCl, 2 mM KCl, 2 mM CaCl$_2$, 1 mM MgSO$_4$, 1 mM NaHCO$_3$ and 0.5 mM NaH$_2$PO$_4$; Sigma-Aldrich) for application. Drug application electrodes were made using either two-barrel or single-barrel glass micropipettes as described previously (Huang *et al.* 2018; Marquez & Chacron, 2018). For single neuron recordings, two-barrel pipettes were used for independent application of serotonin or glutamate in the vicinity of the neuron being recorded. We relied on glutamate-elicited excitatory responses to verify that the pipette was correctly placed next to the neuron we were recording from, as done previously (Deemyad *et al.* 2013; Huang *et al.* 2018; Marquez & Chacron, 2018). For behavioural experiments, single-barrel pipettes were used for bilateral application of serotonin in the lateral segment of the ELL. Drugs were delivered using a picospritzer at 15–25 p.s.i. during 100 ms, as done previously (Deemyad *et al.* 2013; Huang *et al.* 2018; Marquez & Chacron, 2018). We note that previous studies have shown that application of saline alone in this manner does not significantly alter either ELL pyramidal cell activity or behaviour (Deemyad *et al.* 2013; Huang *et al.* 2016).

Electrophysiology

Extracellular recordings from ELL pyramidal cells were obtained with metal-filled micropipettes (Frank & Becker, 1964) using standard methodology (Huang *et al.* 2018). Recordings from $n = 17$ pyramidal cells in $N = 10$ fish were included in this study. Based on recording depth and mediolateral placement of the electrode, pyramidal cells recorded were located within the lateral segment of the ELL. We chose this segment as it receives the greatest amount of serotonergic innervation (Deemyad *et al.* 2011). All recordings were amplified (A-M Systems 1700, Calsborg, WA, USA), digitized at 10 kHz sampling rate (CED 1401; Spike2 version 8.1 software; Cambridge Electronic Design, Cambridge, UK) and stored for offline analysis.

Behaviour

$N = 7$ fish were used for behavioural experiments. The electric organ discharge (EOD) of *A. leptorhynchus* is neurogenic and therefore is not affected by injection of curare. In this study, behavioural responses consist of modulations of the EOD frequency. The animal's EOD signal was recorded through a pair of electrodes located on either side of the recording tank parallel to the fish's rostro-caudal axis (Fig. 1*A*). The zero crossings of the EOD signal were detected and low-pass filter (second order Butterworth filter with 0.05 Hz cut-off frequency) to obtain the time-varying EOD frequency as described previously (Huang *et al.* 2018).

Stimulation

A 100 s baseline period was recorded in the absence of stimulation before stimulus presentation for both neurons and behaviour. All stimuli consisting of amplitude modulations (AMs) of the animal's own EOD were produced by triggering a function generator to emit 1 cycle of a sine wave for each zero crossing of the EOD, as done previously (Bastian *et al.* 2002). The frequency of the emitted sine wave was set slightly higher ($\sim$40 Hz) than that of the animal's own EOD, which allowed the output of the function generator to be synchronized to the animal's discharge. The emitted sine wave was subsequently multiplied with the desired AM waveform (MT3 multiplier; Tucker Davis Technologies, Alachua, FL, USA), and the resulting signal was isolated from ground (A395 linear stimulus isolator; World Precision Instruments, Sarasota, FL, USA). The isolated signal was then delivered through a pair of chloridized silver wire electrodes placed 15 cm away from the animal on either side of the recording tank perpendicular to the fish's rostro-caudal axis (Fig. 1*A*). The resulting signal measured at the fish's skin was approximated using a dipole (1 mm

distance between the two poles) positioned next to the fish 2 mm away. For both neural recordings and behavioural experiments, our stimuli consisted of 5–15 Hz noise carrier waveform (i.e. AM) whose amplitude (i.e. envelope) varied sinusoidally at frequencies ranging from 0.05 to 1 Hz. In

order to test neural responses to AM signals, we used a noise stimulus containing AM carrier frequencies ranging from 5 to 15 Hz as done previously (Huang *et al.* 2018). We also tested behavioural responses to 4 Hz sinusoidal AM stimulation as done previously (Deemyad *et al.* 2013). Briefly, the 4 Hz sinusoidal AM stimulus with 50 s duration was presented five times with a rest period of at least 50 s between each presentation.

Terminal procedures

Animals were euthanized by anaesthetic overdose (MS-222) followed by decapitation as per approved protocol 5285 and according to the guidelines of the Canadian Council on Animal Care.

Data analysis

Analysis of neural and behavioural responses to envelopes was performed using standard methodology that relates the sinusoidal envelope stimuli to either the spiking activities of neurons or the time-varying EOD frequency (Metzen & Chacron, 2014; Huang *et al.* 2016; Huang *et al.* 2018).

Baseline firing rates and burst fractions were calculated from 100 s of baseline activity before stimulus presentation. A burst threshold of 10 ms was used to separate the full spike train into the burst train and the isolated spike train, as indicated by the trough of the bimodal interspike interval (ISI) distribution (Oswald *et al.* 2004; Ellis *et al.* 2007; Khosravi-Hashemi *et al.* 2011; Khosravi-Hashemi & Chacron, 2012; Deemyad *et al.* 2013; Khosravi-Hashemi & Chacron, 2014; Marquez & Chacron, 2018). Specifically, if an ISI was less than the threshold, then the two action potentials were deemed to be part of a burst; if the next ISI was also less than the threshold, then the third action potential was also deemed to be part of the same burst. This process continues until the ISI is greater than the threshold. The isolated spike train consists of spikes that were not part of bursts. Burst fraction was defined as the ratio of the number of spikes that belong to a burst to the total number of spikes.

Responses to noise AMs were measured using standard techniques. Specifically, we computed the spike-triggered average (STA) by averaging stimulus segments during 1 s windows centred at the action potential times. Thus, the STA is given by $\langle S(t - t_i) \rangle$ where $S(t)$ is the AM carrier and $\langle \ldots \rangle$ denotes averaging over the spike times t_i. The STA amplitude was calculated as the difference between the maximum and minimum values of the STA. To further estimate the response sensitivity to noise AMs, we constructed a binary sequence from the spike times using bins of 0.1 ms width. These were obtained by setting the value of a given bin to 1 if an action potential occurred during that bin and to zero otherwise. We note that the value of any given bin can be only 0 or 1 because
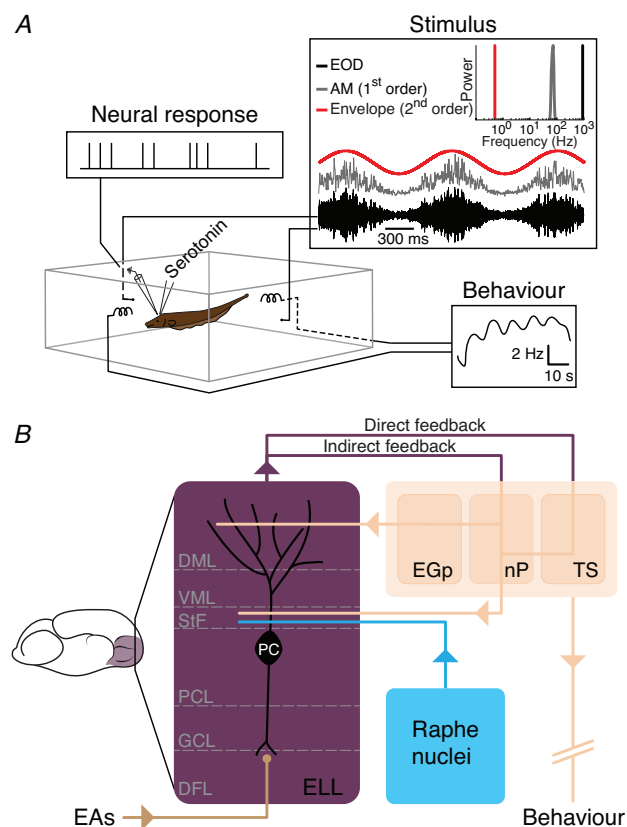

Figure 1. Experimental set-up and relevant anatomy and circuitry of the electrosensory system

A, diagram showing the awake-behaving preparation where the fish is immobilized and neural and behavioural responses are recorded while the stimulus is presented before and after exogenous serotonin application. Stimuli consisted of a noisy AM (first order) whose amplitude (envelope or second order) was modulated sinusoidally at different frequencies. Example traces of such signals are displayed with their respective frequency contents. *B*, simplified circuitry of the electrosensory system. Sensory information travels from electroreceptor afferents (EA) in the skin to pyramidal cells located in the electrosensory lateral line lobe (ELL) within the hindbrain. Information is then integrated and sent to higher brain areas where further processing occurs to eventually give rise to behavioural responses. In addition, ELL pyramidal cells receive two sources of glutamatergic feedback input, one directly from nP and another indirectly from EGp, as well as serotonergic modulatory input from the raphe nuclei. Our original study investigated the role of glutamatergic feedback in determining envelope responses (Huang *et al.* 2018); here we investigated the role of serotonergic feedback. Approximate laminae positions are shown: DFL, deep fibre layer; DML, dorsal molecular layer; GCL, granule cell layer; PCL, pyramidal cell layer; StF, stratum fibrosum; VML, ventral molecular layer. Other abbreviations: EGp, eminentia granularis posterior; nP, nucleus praeminentialis; TS, torus semicircularis. [Colour figure can be viewed at wileyonlinelibrary.com]

the bin width is less than the absolute refractory period of the neurons considered in this study (Toporikova & Chacron, 2009). The neural sensitivity to the AM carrier was then computed as: $G(f) = |P_{sr}(f)|/P_{ss}(f)$, where $P_{sr}(f)$ is the cross-spectrum between the stimulus and the binary sequence, and $P_{ss}(f)$ is the power spectrum of the stimulus. To estimate spectral quantities, we used multitaper techniques with eight Slepian tapers using the MATLAB (The Mathworks, Natick, MA, USA) functions 'cpsd' and 'pwelch', as done previously (Huang *et al.* 2018). Since our estimates of neural sensitivity $G(f)$ did not vary with frequency within the AM stimulus frequency range (i.e. 5–15 Hz), we quantified neural sensitivity by taking the value at 10 Hz.

To quantify neural responses to envelopes, we used linear systems identification techniques. Specifically, the neural gain was calculated as the ratio of the amplitude of the modulated firing rate response and the amplitude of the stimulus obtained from the dipole during the recording. To determine the firing rate modulation, we computed the phase histogram (i.e. the time-dependent firing rate averaged over the envelope cycles) and fitted a sinewave as done previously (Huang & Chacron, 2016; Huang *et al.* 2018). The response phase was calculated as the average phase at which the fitted sinewave reached its maximum value relatively to the maximum value of the stimulus waveform. Data obtained from ON- and OFF-type ELL pyramidal neurons were pooled as previous studies have consistently reported that there is no overall difference between their responses to envelopes (Huang & Chacron, 2016; Huang *et al.* 2018).

We fitted a power law to the neural gain as a function of frequency curve to obtain the neural exponent α_{neuron}. To quantify how changes in α_{neuron} affect optimal coding, we used linear response theory (Risken, 1996), which assumes that the response power spectrum is equal to the absolute value of the gain squared times the stimulus power spectrum (Huang *et al.* 2016). In this case, the optimal stimulus power is proportional to the inverse neural gain squared as a function of frequency. Further, the power law exponent at which stimulus power decays, α_{stim}, is then given by $-2\alpha_{neuron}$.

Behavioural responses. We first recorded the jamming avoidance response (JAR) in response to 4 Hz sinusoidal AM stimulation as mentioned above. The JAR magnitude was defined as the maximum EOD frequency elicited during stimulation relative to the EOD frequency baseline value. JAR responses were averaged across stimulus presentations and compared before and after serotonin application as done previously (Deemyad *et al.* 2013).

Behavioural responses to sinusoidal envelopes were quantified using linear systems identifications techniques (Metzen & Chacron, 2014). Thus, the gain was defined as the ratio of the EOD frequency peak-to-peak amplitude

to that of the envelope stimulus, the phase is the amount of time relative to the envelope cycle that EOD frequency must be shifted by in order to be in phase with the sinusoidal envelope stimulus, and the offset is the difference between the mean EOD frequency during stimulation and that obtained prior to stimulation (i.e. during baseline).

Statistics

All values are reported as means $\pm$ SD throughout. Statistical significance was evaluated through either a parametric Student's *t* test or a non-parametric Wilcoxon's signed-rank test for paired measurements at the $P = 0.05$ level. The choice of test was based on whether the data followed a normal distribution (parametric test) or not (non-parametric test), as assessed by a Lilliefors test. For multiple comparisons, statistical significance was assessed through a one-way ANOVA at the $P = 0.05$ level. Correlations were calculated using Pearson's correlation coefficient. For the whisker boxplots, the central mark indicates the median and the bottom and top edges indicate the 25th and 75th percentiles, respectively. Whiskers extend to the values that are not considered outliers. All data points including outliers are plotted individually.

Results

To investigate how serotonin influences neural and behavioural responses to envelope stimuli, we first recorded the activity of pyramidal cells in response to envelopes before and after exogenous serotonin application. The experimental set-up is illustrated in Fig. 1*A*. The stimuli consisted of noisy EOD amplitude modulations (AMs, first order) whose amplitude (envelope, second order) varied sinusoidally at different frequencies (Fig. 1*A*, top right panel). It is important to note that the first- and second-order features of the stimulus correspond to second- and third-order features of the actual signal received by the animal, respectively. Figure 1*B* shows the relevant circuitry studied. Pyramidal cells receive feedforward input from electro-receptors (EAs) and are the main output neurons of the ELL that project to higher brain areas, thereby giving rise to behaviour. ELL pyramidal cells also receive large amounts of glutamatergic and/or GABAergic feedback from higher brain areas (Fig. 1*B*) as well as neuro-modulatory serotonergic feedback from the raphe nuclei (Fig. 1*B*).

Serotonin enhances neural responses to envelopes through burst firing

We initially compared ELL pyramidal cells' baseline activity (i.e. a 100 s period in the absence of stimulation but in the presence of the animal's unmodulated EOD)

before and after exogenous serotonin application through a double-barrel pipette. It should be noted that this technique delivers serotonin focally within the vicinity of the neuron being recorded (Bastian, 1993; Deemyad *et al.* 2013) (see Methods). Serotonin application significantly increased excitability and caused increased firing of bursts (i.e. packets of action potentials followed by quiescence) under baseline activity (Fig. 2*A*). We used a threshold that was located at the trough of the bimodal interspike interval (ISI) distribution (Fig. 2*B* and *C*) in order to separate the spike train into bursts and isolated spikes (Oswald *et al.* 2004; Khosravi-Hashemi *et al.* 2011) (see Methods). Serotonin application significantly increased both the mean firing rate and the burst fraction (i.e. the fraction of action potentials belonging to bursts, see Methods) under baseline activity (Fig. 2*D* and *E*).

We next investigated how serotonin application affected ELL pyramidal cell responses to stimulation. Analysis of responses to the AM carrier revealed an increase in the spike triggered average (STA, which is the average stimulus waveform around the action potential time; see Methods; Fig. 3*A*). We quantified this increase by computing the STA amplitude (i.e. the difference between the maximum and minimum values of the STA; see Methods) and found a significant increase after serotonin application (Wilcoxon's signed-rank test, $P = 84 \times 10^{-4}$, $n = 17$; Fig. 3*B*). Further analysis revealed that the increase in the STA was most likely due to an increase in the neural sensitivity to the stimulus (Fig. 3*C*), which also increased significantly after serotonin application (Wilcoxon's signed-rank test, $P = 0.012$, $n = 17$; Fig. 3*D*). Overall, these results are consistent with previous ones showing increased response to low frequency AM after serotonin application (Deemyad *et al.* 2013).

We next investigated the effects of serotonin application (Fig. 4*A*) on ELL pyramidal cell responses to envelopes. We found that, under control condition (Fig. 4*B*), ELL pyramidal cells responded to envelopes through modulations in firing rate (Fig. 4*B*, black). Separating the spike train into bursts and isolated spikes revealed that this modulation was primarily due to bursts rather than isolated spikes (Fig. 4*B*, compare black to dashed and solid grey). This is because the firing rate modulations seen for bursts were largely in phase with those seen for all spikes (Fig. 4*B*, compare black and dashed grey) whereas those seen for isolated spikes were smaller in amplitude and mostly out of phase (Fig. 4*B*, compare black and solid grey). After serotonin application (Fig. 4*C*), ELL pyramidal cells continued to respond to envelopes through modulations in firing rate that were overall higher in amplitude than under control conditions when considering all spikes (compare Fig. 4*C* to Fig. 4*B*). Separating the spike train into bursts and isolated spikes revealed that this modulation was primarily due to bursts rather than isolated spikes (Fig. 4*C*, compare cyan to

dashed blue and light blue). This is because the firing rate modulations seen for bursts were largely in phase with those seen for all spikes (Fig. 4*C*) whereas those seen for isolated spikes were smaller in amplitude (Fig. 4*C*).

We quantified the neural responses from all spikes, bursts and isolated spikes to different sinusoidal envelope frequencies using linear systems identification techniques
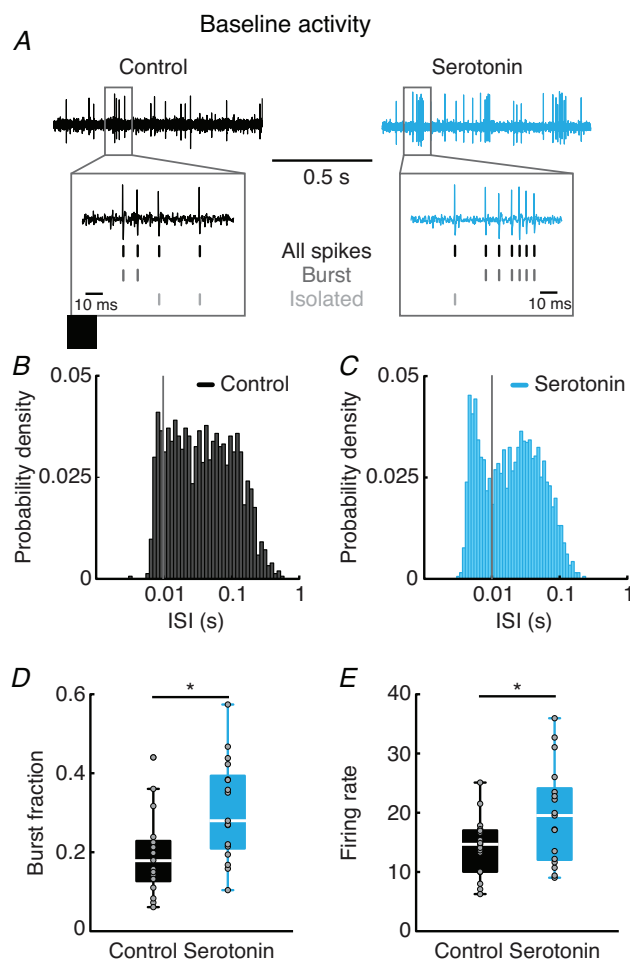

Figure 2. Serotonin increases ELL pyramidal cell excitability during spontaneous activity
A, spiking activity of a representative neuron before (left) and after (right) serotonin application in the absence of stimulation. Insets show spikes detected offline and classified as belonging to a burst or isolated spike according to their interspike interval (ISI). An ISI of 10 ms was chosen as minimum interval between burst spikes (see Methods). *B*, ISI histogram from a typical ELL pyramidal cell in the absence of stimulation during control condition. *C*, same as *B* but after serotonin application; note that a bipolar distribution is more clearly distinguished after serotonin application. Vertical lines indicate the chosen burst threshold of 10 ms. *D*, burst fraction (i.e. the number of spikes that belong to a burst, see Methods) in the absence of stimulation before (left) and after (right) serotonin application ($P = 7.04 \times 10^{-7}$, Student's *t* test, $n = 17$). *E*, firing rate in the absence of stimulation before (left) and after (right) serotonin application ($P = 8.09 \times 10^{-7}$, Student's *t* test, $n = 17$). *Statistical significance at the $P = 0.05$ level as quantified by Student's *t* test. [Colour figure can be viewed at wileyonlinelibrary.com]

(see Methods). We found that the neural tuning curve (i.e. the neural gain as a function of frequency) was high-pass. Indeed, the neural gain increased as a power law with increasing frequency under control conditions (Fig. 4*D*). The best-fit power law exponent for our dataset was $\alpha_{neuron} = 0.38 \pm 0.29$ (Fig. 4*D*, inset, black). We found that serotonin application primarily increased neural sensitivity to envelopes with frequencies ≥ 0.5 Hz (Fig. 4*D*). As a result, the neural tuning curve after serotonin application increased more steeply with increasing envelope frequency than under control conditions, as quantified by a significantly greater power law exponent (Fig. 4*D*, inset). Qualitatively different results were seen when looking at bursts and isolated spikes. Indeed, the neural gain computed from bursts significantly increased for all but the lowest frequency (Fig. 4*E*). Increases in gain were much more prominent than for all spikes and were greater for higher than for lower frequencies, such that the best-fit power law exponent significantly increased after serotonin application (Fig. 4*E*, inset). Overall, neural gain values computed from isolated spikes were not significantly

altered by serotonin application with the exception of a small increase for frequencies 0.2 and 0.75 Hz and a bigger increase for the highest frequency, 1 Hz (Fig. 4*F*), which is qualitatively similar to that observed for all spikes, except that gain values were much lower overall (compare Fig. 4*D–F*). The best-fit power law exponent values for isolated spikes were also not significantly altered (Fig. 3*F*, inset).

We then computed the phase (i.e. the amount of time relative to the envelope cycle that is needed to shift the response such that it is in phase with the envelope; see Methods) for all spikes (Fig. 4*G*), bursts (Fig. 4*H*) and isolated spikes (Fig. 4*I*). While phases were relatively independent of frequency and were not significantly altered by serotonin application, we found that the phases of all spikes, bursts and isolated spikes were significantly different from one another on average (one-way ANOVA, $F_{(2,15)} = 838.36$, $P = 4.06 \times 10^{-16}$). Importantly, the fact that the burst train is much more strongly modulated at a different phase than the isolated spike train leads to only partial destructive interference when summing them to obtain the all-spike train. This explains why the phase obtained from all spikes is much closer to that obtained from the burst train than to that obtained from the isolated spike train.

Increases in burst firing accompanies increased neural gain to envelopes after serotonin application

We next tested as to the underlying mechanism for increased firing rate modulation as quantified by increase neural gain after serotonin application. Our results show that burst fraction increased significantly for all envelope frequencies after serotonin application (Fig. 5*A*). However, we only found significant increases in the all-spike and burst firing rates (Fig. 5*B* and *C*) while there were no significant changes in the isolated spike firing rate (Fig. 5*D*). As such, while there is increased spiking activity after serotonin application, these increases are primarily due to increased burst firing with isolated spike firing remaining mostly constant. Further, when we plotted the relative change in neural gain after serotonin application as a function of the relative change in all-spike rate (Fig. 5*E*), burst rate (Fig. 5*F*) and isolated spike rate (Fig. 5*G*), we found a strong and significantly positive correlation for all spikes and burst spikes, but not for isolated spikes. Therefore, increased burst firing accompanies and likely leads to a greater range of modulation of firing activity and thus a greater gain during stimulation for the burst and all-spike trains.

Serotonin application compromises optimized coding via temporal whitening

As mentioned above, previous results have shown that the tuning properties of ELL pyramidal cells were matched
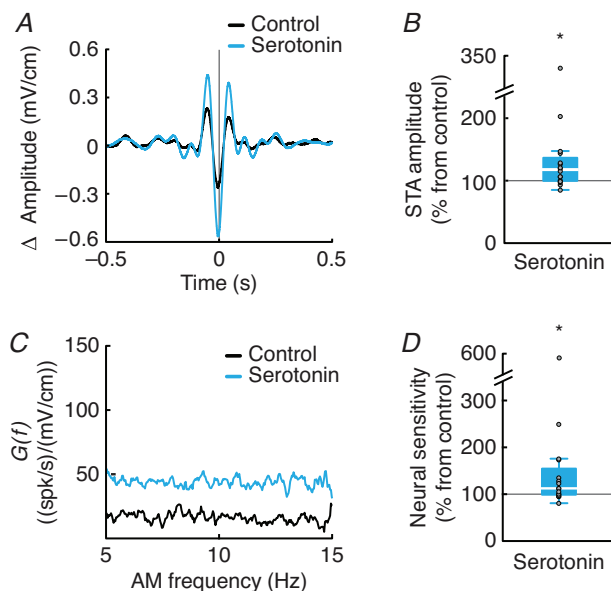
Figure 3. Serotonin increases ELL pyramidal cells sensitivity to the carrier
A, spike-triggered average (STA) of the noisy AM stimulus waveform before (lower amplitude trace) and after (higher amplitude trace) serotonin application for a typical ELL pyramidal cell. *B*, STA amplitude (i.e. the difference between the maximum and minimum STA values) after serotonin application as a percentage relative to control was significantly different from 100% (Wilcoxon's signed-rank test, $P = 84 \times 10^{-4}$, $n = 17$). *C*, neural sensitivity to the noisy AM carrier stimulus for the same representative example cell as in *A* before (bottom) and after (top) serotonin application. *D*, the neural sensitivity to the noisy AM carrier stimulus after serotonin application relative to control was significantly greater than 100% (Wilcoxon's signed-rank test, $P = 0.012$, $n = 17$). [Colour figure can be viewed at wileyonlinelibrary.com]
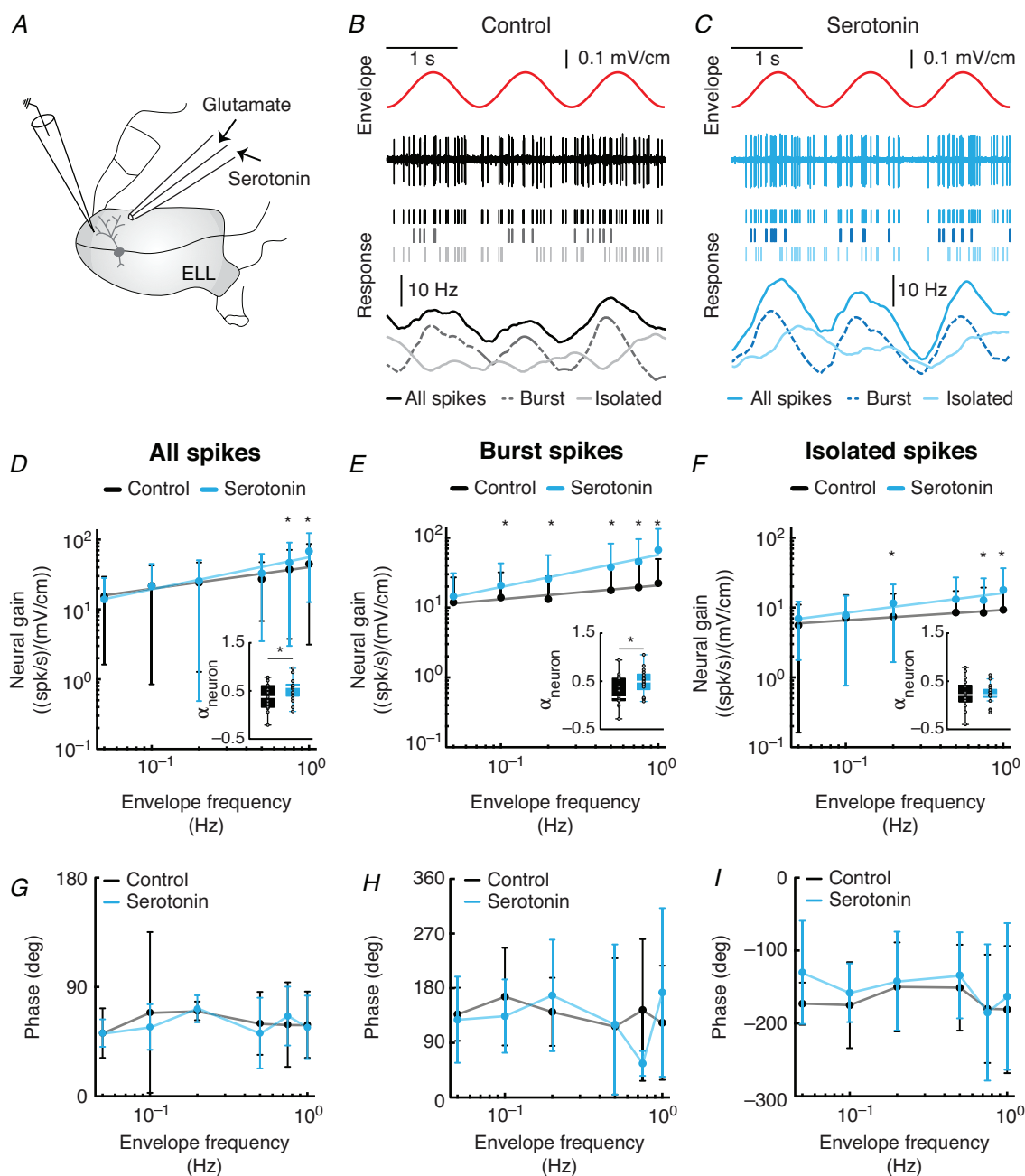
Figure 4. Exogenous serotonin application enhances neural responses to envelopes
A, schematic diagram showing the positioning of the recording electrode within the ELL and a double-barrel pipette used to apply either glutamate (to elicit excitatory responses from pyramidal cells) or serotonin in the vicinity of the recorded neuron. *B*, response to envelopes of a representative neuron during control condition. Top, stimulus waveform (red). Middle, spiking activity of the neuron and detected spikes split into all spikes (black), burst spikes (dashed grey) and isolated spikes (solid grey). Bottom, time-dependent firing rate generated from all spikes, burst and isolated spikes. *C*, same as *B* but after serotonin application. *D*, population averaged tuning curve showing neural gain as a function of envelope frequency before and after serotonin application. The continuous lines show the best power law fits to the data. Inset: population averaged best-fit power law exponents before and after serotonin application ($P = 0.0013$, Student's *t* test, $n = 17$). *E*, same as *D* but showing neural gain computed from burst spikes only ($P = 0.014$, Student's *t* test, $n = 17$). *F*, same as *D* but showing neural gain computed from isolated spikes only ($P = 0.76$, Student's *t* test, $n = 17$). *G*, population averaged phase as a function of envelope frequency before and after serotonin application for all spikes. *H*, same as *G* but for burst spikes. *I*, same as *H* but for isolated spikes. *Statistical significance at the $P = 0.05$ level as quantified by Wilcoxon's signed-rank test or Student's *t* test. [Colour figure can be viewed at wileyonlinelibrary.com]

to natural stimulus statistics such as to optimally encode them via temporal whitening (Huang *et al.* 2016). Specifically, the tuning function (Fig. 6*A*, middle) opposes the decay of the stimulus power (Fig. 6*A*, right), such that the resulting neural response power (Fig. 6*A*, left) is independent of frequency (i.e. temporally whitened). As such, a change in the tuning function is predicted to lead to optimized coding of stimuli with different statistics. Since the results of Huang *et al.* (2016) only considered all spikes, we investigated the contributions of bursts and isolated spikes towards optimized coding under control and after serotonin application.

To do so, we computed the power law exponent α_{stim} characterizing the decay of stimulus spectral power as a
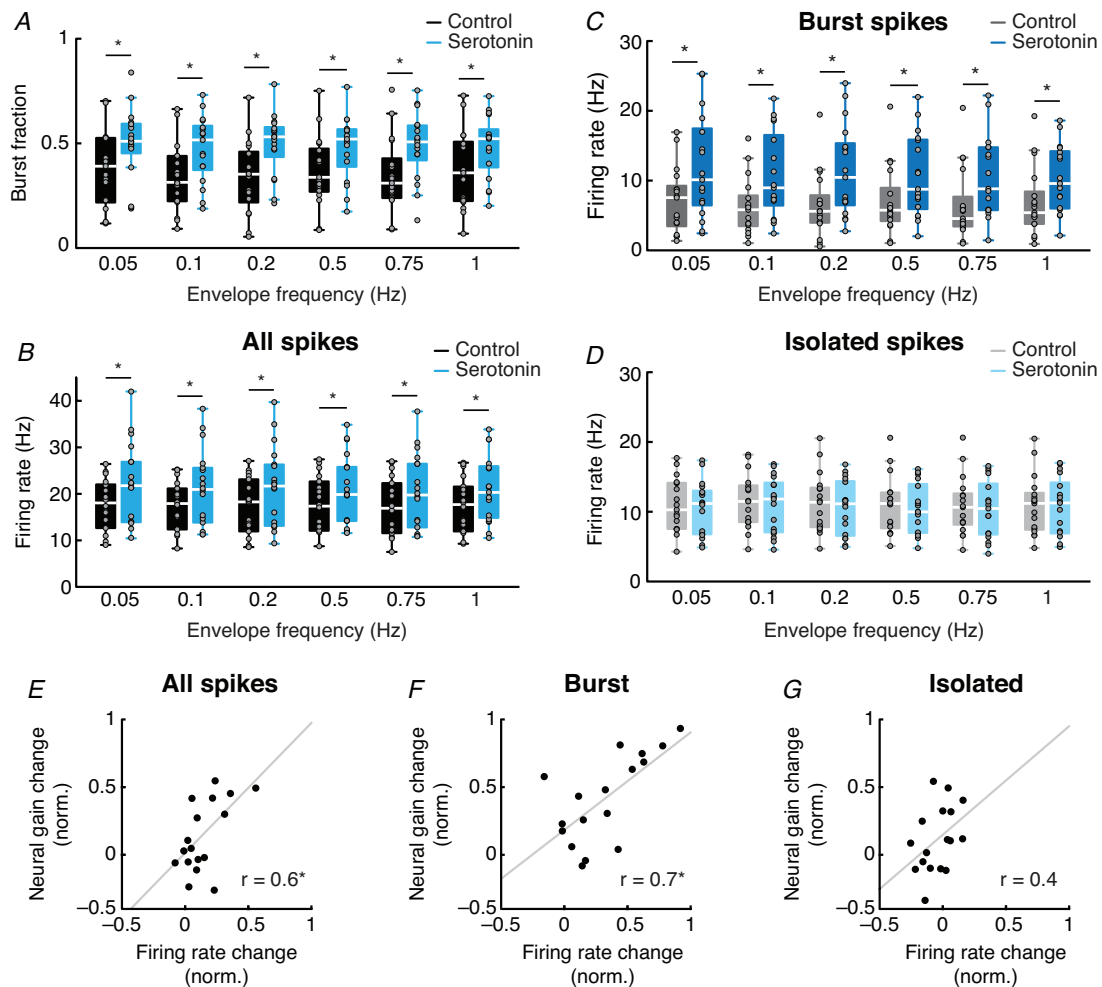

Figure 5. Serotonin-induced increase in bursting activity is correlated with neural gain changes that affect optimized coding of envelopes

A, burst fraction before and after serotonin application computed for all spikes during stimulation with different envelope frequencies (0.05 Hz envelope: $P = 0.025$; 0.1 Hz envelope: $P = 19 \times 10^{-4}$; 0.2 Hz envelope: $P = 12 \times 10^{-4}$; 0.5 Hz envelope: $P = 60 \times 10^{-4}$; 0.75 Hz envelope: $P = 56 \times 10^{-5}$; 1 Hz envelope: $P = 63 \times 10^{-4}$; Student's *t* test for 0.05 Hz envelope, Wilcoxon's signed-rank test for the rest, $n = 17$). *B*, firing rate before and after serotonin application computed for all spikes during stimulation with different envelope frequencies (for all spikes: 0.05 Hz envelope: $P = 0.015$; 0.1 Hz envelope: $P = 0.015$; 0.2 Hz envelope: $P = 64 \times 10^{-4}$; 0.5 Hz envelope: $P = 0.02$; 0.75 Hz envelope: $P = 0.01$; 1 Hz envelope: $P = 0.02$; Student's *t* test, $n = 17$). *C*, same as *B*, but for burst spikes (0.05 Hz envelope: $P = 0.02$; 0.1 Hz envelope: $P = 71 \times 10^{-4}$; 0.2 Hz envelope: $P = 42 \times 10^{-4}$; 0.5 Hz envelope: $P = 8 \times 10^{-3}$; 0.75 Hz envelope: $P = 1.6 \times 10^{-3}$; 1 Hz envelope: $P = 0.011$; Student's *t* test for 0.05, 0.1 and 0.2 Hz envelopes, Wilcoxon's signed-rank test for the rest, $n = 17$). *D*, same as *B*, but for isolated spikes (0.05 Hz envelope: $P = 0.47$; 0.1 Hz envelope: $P = 0.31$; 0.2 Hz envelope: $P = 0.17$; 0.5 Hz envelope: $P = 0.29$; 0.75 Hz envelope: $P = 0.34$; 1 Hz envelope: $P = 0.56$; Student's *t* test, $n = 17$). *Statistical significance at the $P = 0.05$ level as quantified by either Student's *t* test or Wilcoxon's signed-rank test. *E*, relative neural gain change as a function of the relative change in firing rate during stimulation for all spikes. The continuous line shows the best linear fit to the data ($r = 0.59$, $P = 0.013$, $n = 17$). *F*, same as *E* but for burst spikes ($r = 0.67$, $P = 32 \times 10^{-4}$, $n = 17$). *G*, same as *E* but for isolated spikes ($r = 0.41$, $P = 0.1$, $n = 17$). [Colour figure can be viewed at wileyonlinelibrary.com]

function of increasing frequency that is optimally encoded by a neural tuning function that increases as a power law with exponent α_{neuron}, such that the response power is independent of frequency (see Methods). Under control conditions, we found that the power spectrum of the stimulus that leads to optimal coding when considering the full spike train decayed with an exponent α_{stim} whose value agreed with that found under naturalistic conditions (Fig. 6*B*, black, compare with horizontal line in bottom panel). However, after serotonin application, the increase in α_{neuron} (Fig. 4*D*) led to a steeper decrease of

stimulus power as characterized by more negative values of α_{stim} (Fig. 6*B*, compare with horizontal line in bottom panel). We next computed α_{stim} for bursts and isolated spikes. For bursts, our results show that, under control conditions, the power spectrum of the stimulus that leads to optimal coding decayed less steeply than for all spikes (Fig. 6*C*, black, compare with Fig. 6*B*, black), thereby leading to values of α_{stim} that were higher than those found under naturalistic conditions (Fig. 6*C*, bottom panel). In contrast, after serotonin application, the power spectrum of the stimulus that leads to optimal coding
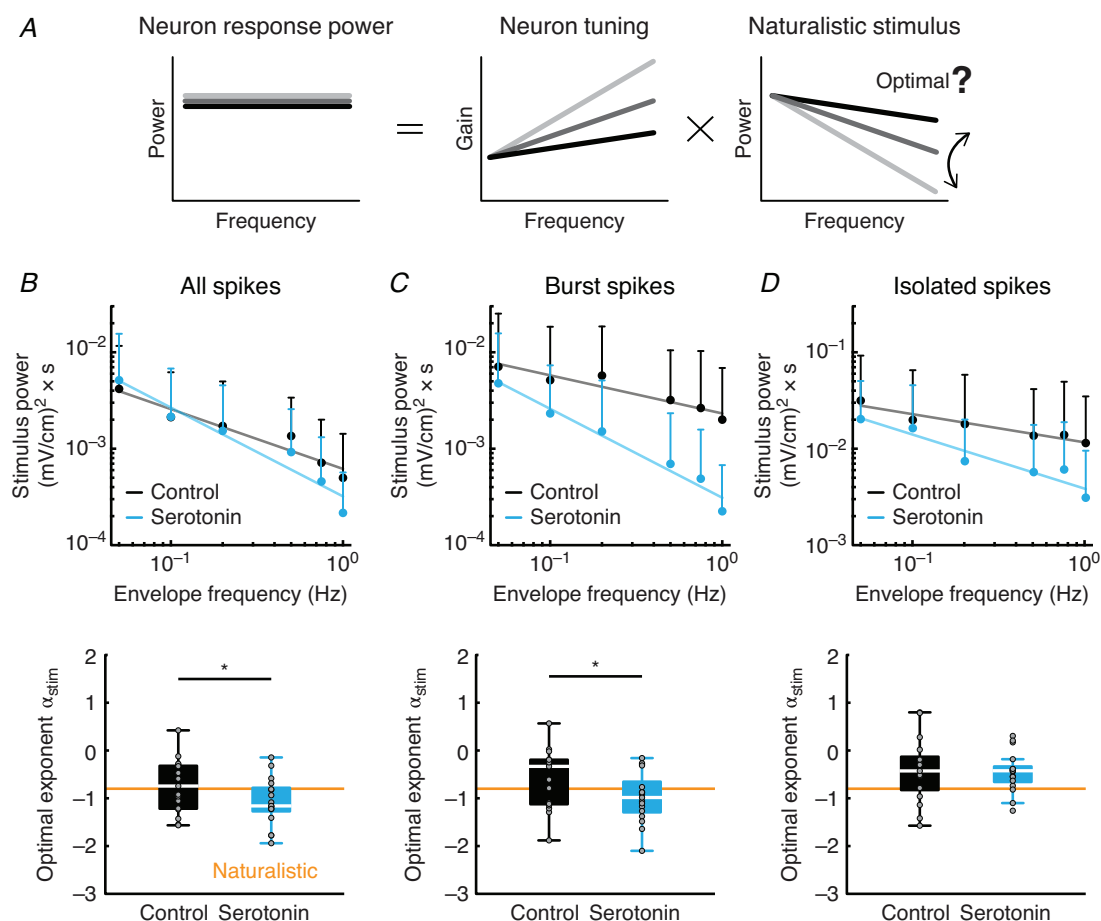

Figure 6. Serotonin application alters the power law exponent at which stimulus power decays in order for coding to remain optimal
A, schematic representation of how the tuning function (middle) must be matched to natural stimulus statistics (right) in order for the neural response power to be independent of frequency (left). Different tuning functions (grey lines, middle panel) all give rise to optimal coding (grey lines, left panel) of stimuli with different statistics (grey lines, right panel). *B*, top, population averaged stimulus power that gives rise to optimal coding as a function of envelope frequency before and after serotonin application. The continuous lines show the best power law fits to the data. Bottom, population-averaged optimal exponent α_{stim} (see Methods) for which optimal coding is achieved under control and after serotonin application for all spikes were significantly different from one another ($P = 13 \times 10^{-4}$, Student's *t* test, $n = 17$). The horizontal line indicates the value of -0.8, which is the power law exponent of the stimuli that the fish experience under naturalistic conditions as reported previously (Metzen & Chacron, 2014). *C*, same as *B*, but for burst spikes only. The values of α_{stim} obtained under control and after serotonin application were significantly different from one another ($P = 14 \times 10^{-3}$, Student's *t* test, $n = 17$). *D*, same as *B*, but for isolated spikes only. Note that values of α_{stim} obtained under control and after serotonin application were not significantly different from one another ($P = 0.76$, Student's *t* test, $n = 17$). *Statistical significance at the $P = 0.05$ level as quantified by Student's *t* test. [Colour figure can be viewed at wileyonlinelibrary.com]

decayed more steeply similar to that seen for all spikes (compare Fig. 6*C* to Fig. 6*B*), as reflected by α_{stim} values that were similar to those seen for all spikes (compare bottom panel of Fig. 6*C* to bottom panel of Fig. 6*B*) and thus lower than those found under naturalistic conditions (Fig. 6*C*, compare with horizontal line in bottom panel). For isolated spikes, our results show that the power spectra of the stimuli that led to optimal coding decayed similarly both under control conditions and after serotonin application (Fig. 6*D*, upper panel), as reflected by α_{stim} values that were similar to but higher than those seen under naturalistic conditions (Fig. 6*D*).

As such, our results show that serotonin application disrupts optimal coding by all spikes by shifting the exponent of the optimal stimulus to lower values (Fig. 6*B*). Separating the spike train into bursts and isolated spikes revealed that this is because the optimal exponent α_{stim} for bursts also shifted to similar values, as the exponent for isolated spikes did not change. This makes sense as, after serotonin application, bursts comprise a greater fraction of the spike train as quantified by increased burst fraction. The consequences of these results for optimal coding and the role of serotonin towards optimizing coding of stimuli encountered during particular behavioural contexts are discussed below.

Serotonin enhances behavioural responses to envelopes

We lastly investigated the effects of serotonin application on behaviour (Fig. 7*A*). We first tested that serotonin application was effective by measuring the animal's jamming avoidance response (JAR) before and after application. The JAR occurs when a fish changes its EOD frequency during the encounter with another fish with similar EOD frequency to prevent jamming of their electric signals (Heiligenberg, 1991). JAR magnitude significantly increased after serotonin application (Fig. 7*B* and *C*), indicating that our serotonin application was effective. We next tested the effects of serotonin application on behavioural responses to envelope stimuli by measuring the animal's ability to track the stimulus through changes in its EOD frequency. This behavioural response is well-characterized (Metzen & Chacron, 2014) and is strongly influenced by ELL pyramidal cell responses (Huang & Chacron, 2016; Huang *et al.* 2016, 2018). Such behavioural responses consist of a positive offset in EOD frequency around which the EOD frequency varies sinusoidally (Fig. 7*D*). We used linear systems identification techniques (see Methods) to quantify both the gain and phase in the behavioural response (Fig. 7*D*), similar to what was done previously for neural activity. We found that the animal's EOD frequency tracked the envelope stimulus with greater amplitude and offset following serotonin application (Fig. 7*D*, compare black
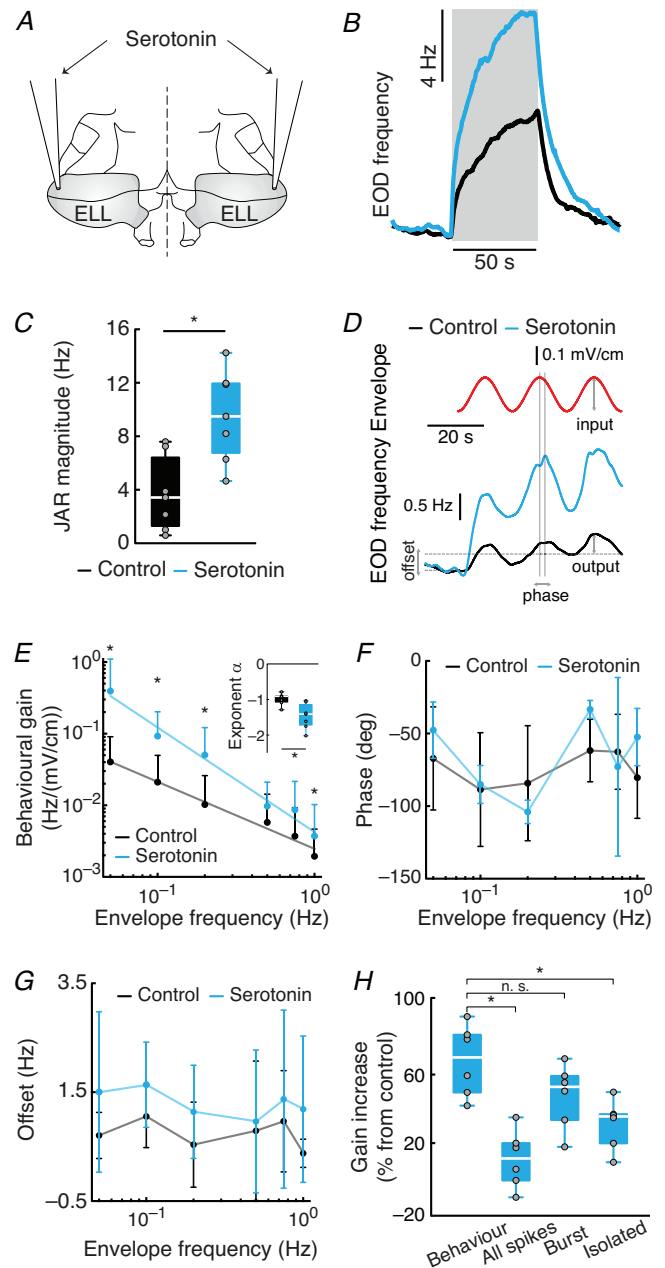

Figure 7. Serotonin enhances behavioural responses to envelopes

A, schematic representation of the bilateral positioning of single barrel pipettes used to apply serotonin within the ELL. *B*, time course of the EOD frequency of a representative fish before (bottom) and after (top) serotonin application showing the JAR when the stimulus is presented (grey box, see methods). *C*, population averaged JAR magnitude before (black) and after (blue) serotonin application. The JAR magnitude after serotonin application was significantly different from control as tested by Student's *t* test ($P = 33 \times 10^{-4}$, $n = 7$). *D*, top, stimulus waveform (red). Bottom, time-dependent EOD frequency of a representative fish during stimulation before (bottom) and after (top) serotonin application. Grey lines indicate the parameters used to characterize the behavioural responses to envelopes: the offset is defined as the difference between the baseline EOD frequency and the mean EOD frequency during stimulation (dashed grey lines), the phase is defined as the time shift

and blue). We next varied the envelope frequency and computed behavioural sensitivity, phase and offset. We found that, under control conditions, behavioural sensitivity decreased as a power law as a function of increasing envelope frequency (Fig. 7*E*, black). However, after serotonin application, behavioural sensitivities to low envelope frequencies (i.e. <0.5 Hz) were most increased. As a result, the behavioural sensitivity decreased more steeply with increasing envelope frequency (Fig. 7*E*), as quantified by a significantly more negative power law exponent (Fig. 7*E*, inset). There were no significant changes in phase (Fig. 7*F*), but we observed that offset values significantly increased after serotonin application (Fig. 7*G*).

How do changes in neural gain relate to changes in behavioural gain? In order to answer this question, we compared relative changes in neural gain using all spikes, bursts and isolated spikes to relative changes in behavioural gain (Fig. 7*H*). Overall, we found that relative changes in neural gain computed from bursts, but not from either of all spikes or isolated spikes, could account for changes in behavioural sensitivity (Fig. 7*H*). This, together with the fact that neural gains computed from bursts were much higher than that computed from isolated spikes, provides evidence that changes in burst firing contribute to changes in behaviour in the electrosensory system. This is further discussed below.

Discussion

Summary of results

We investigated how serotonergic feedback influenced neural and behavioural responses to envelope stimuli.

between the peak of the envelope and the peak of the response (vertical grey lines) normalized to the stimulus period, and gain is defined as the ratio of the response amplitude (output) to the stimulus amplitude (input, grey vertical arrows). *E*, population averaged behavioural sensitivity quantified by behavioural gain as a function of envelope frequency before and after serotonin application. The continuous lines show the best power law fits to the data. Inset: population averaged best fit power law exponents before and after serotonin application ($P = 86 \times 10^{-4}$, Student's t test, $n = 7$). *F*, phase as a function of envelope frequency before and after serotonin application. *G*, offset as a function of envelope frequency before and after serotonin application. Note that offset values after serotonin application are significantly different from those obtained during control conditions (one-way ANOVA test, $F_{(1,10)} = 14.81$, $P = 32 \times 10^{-4}$). *Statistical significance at the $P = 0.05$ level as quantified by a one-way ANOVA. *H*, population averaged gain increases after serotonin application computed for behavioural responses and neural responses as split into all spikes, burst and isolated spikes. Behavioural gain increases are significantly different from neural gain increases computed from all and isolated spikes but not those computed from burst spikes (one-way ANOVA, $F_{(3,20)} = 11.23$, $P = 2 \times 10^{-4}$). [Colour figure can be viewed at wileyonlinelibrary.com]

At the level of ELL pyramidal cells, exogenous serotonin application gave rise to increased burst firing. Interestingly, neural tuning computed from all spikes only increased significantly for the highest envelope frequencies whereas no significant effect was observed when only considering isolated spikes. This is because, when only considering burst spikes, much greater increases in neural sensitivity were observed for all frequencies. Further analysis revealed that serotonin application compromised optimized coding of stimuli whose statistics match those seen under naturalistic conditions. This is because the predicted power spectrum of the stimulus that leads to optimized coding decayed more steeply, as quantified by a more negative power law exponent. Separating the spike train into bursts and isolated spikes revealed that this change was due to the former and not the latter. Serotonin application strongly increased behavioural responses as quantified by increased sensitivity for all frequencies. Comparison of changes in neural and behavioural sensitivities induced by serotonin application revealed that those observed when considering burst spikes were the best predictor of behaviour.

Effects of serotonergic feedback on electrosensory processing

Previous studies have shown that serotonin selectively increases ELL pyramidal cell responses to stimuli that elicit glutamatergic/GABAergic feedback input including low frequency AMs, electrocommunication stimuli (chirps) and also, under certain conditions, looming and receding objects (Deemyad *et al.* 2013; Marquez & Chacron, 2018). Our results show that serotonin also enhances neural and behavioural responses to envelope stimuli and thus provide further confirmation of this hypothesis. This is because previous studies have shown that feedback pathways are a strong determinant of ELL pyramidal cell responses to envelopes (Huang *et al.* 2018; Metzen *et al.* 2018).

What are the mechanisms by which serotonin increases ELL neural responses to envelopes? The effects of exogenous serotonin application on both neural activity and behaviour were similar to those obtained by endogenous release via electrical stimulation of serotonergic pathways (Deemyad *et al.* 2013). This suggests that serotonergic pathways onto ELL pyramidal cells have a unique mode of action and thus most likely a unique function. Previous studies have shown that activation of serotonergic input both *in vitro* (Deemyad *et al.* 2011) and *in vivo* (Deemyad *et al.* 2013) increases pyramidal cell excitability by inhibiting small conductance calcium-activated (SK) potassium channels via 5-HT2-like receptors (Larson *et al.* 2014), which reduces the afterhyperpolarization (AHP) following each

action potential and thus promotes the firing of packets of action potentials followed by quiescence (i.e. 'bursts'). Burst firing in ELL pyramidal cells is mediated by an intrinsic mechanism that relies on an interplay between somatic and dendritic sodium channels (Lemon & Turner, 2000). Specifically, somatic action potentials backpropagate into the dendrites where they can trigger dendritic action potentials that propagate back to the soma, giving rise to a depolarizing afterpotential which promotes excitability and further action potential firing. The depolarizing afterpotential potentiates throughout burst firing, which shortens the ISI. Burst firing terminates when the ISI becomes shorter than the dendritic refractory period (i.e. a 'dendritic failure') (Noonan *et al.* 2003). By inhibiting SK channels and thereby reducing the AHP, serotonergic input thus prevents early burst termination and promotes 'full length' bursts that terminate with dendritic failures (Toporikova & Chacron, 2009; Deemyad *et al.* 2013). The effects of activation of 5-HT2 receptors on ELL pyramidal cell responses to envelopes are most likely due to alterations in how their apical dendrites integrate glutamatergic/GABAergic feedback inputs. This is because feedback inputs, which strongly determine ELL pyramidal cell responses to envelopes (Huang *et al.* 2018; Metzen *et al.* 2018), terminate on their apical dendrites (Sas & Maler, 1983, 1987; Berman & Maler, 1999; Deemyad *et al.* 2011). Interestingly, the effects on responses to envelopes were mostly seen only when considering burst spikes. This is very much unlike the effects of glutamatergic/GABAergic feedback pathways which were observable when considering the full spike trains (Huang *et al.* 2018; Metzen *et al.* 2018). As such, the mechanisms by which serotonergic feedback alters ELL pyramidal cell responses to envelopes most likely differ from those of glutamatergic/GABAergic feedback pathways. Further studies are needed to understand this discrepancy.

Burst firing is seen ubiquitously across sensory systems (see (Krahe & Gabbiani, 2004) for review) and many functional roles have been uncovered that include feature detection (Gabbiani *et al.* 1996; Kepecs & Lisman, 2003; Oswald *et al.* 2004), enhancing the signal-to-noise ratio (Lisman, 1997). In the electrosensory system, burst firing by ELL pyramidal cells can signal low frequency AMs (Oswald *et al.* 2004), electrocommunication stimuli (Marsat & Maler, 2012) and object distance (Clarke *et al.* 2015*b*). However, how burst firing by ELL pyramidal cells encodes envelope stimuli in the electrosensory system had not been considered prior to this study. Our results are thus the first to show that the tuning of burst firing to envelope stimuli is actually more high-pass than that of isolated spikes, which is the opposite of that seen for AMs where bursts primarily encode low frequencies while isolated spikes encode high frequencies (Oswald *et al.* 2004; Avila-Akerberg *et al.* 2010). Moreover, our

results show that the changes in ELL pyramidal cell response properties induced by serotonin application when only considering burst spikes were a much better predict of the resulting changes in behaviour then when considering all spikes or only isolated spikes. As such, our results are the first to provide evidence that burst firing by ELL pyramidal cells is behaviourally relevant. While there is evidence that burst firing induces behaviour in invertebrates (Marsat & Pollack, 2006; McMillan & Grey, 2015), such evidence is lacking in vertebrate systems and, to our knowledge, our current results provide the strongest evidence to date that burst firing in ELL pyramidal cells is actually decoded by downstream areas in order to give rise to behaviour. However, further studies are needed in order to understand how information transmitted by the ELL pyramidal cell population through burst firing is decoded downstream. Indeed, comparison of the effects of serotonin on neural responses through burst firing and behavioural responses revealed important differences. Specifically, increases in neural sensitivity for bursts was minimal at low frequencies and highest for high frequencies, while increases in behavioural sensitivity were instead highest for low frequencies and negligible for higher frequencies. Thus, our results indicate that, while increases in burst firing are in general accompanied by increases in behavioural sensitivity, there is no one-to-one relationship when considering frequencies individually. We hypothesize that such differences are due to significant processing by downstream brain areas. Specifically, frequency-dependent changes in behavioural sensitivity most likely originate from differences in how the activities of ELL pyramidal cell are decoded downstream. Importantly, previous studies have shown that ELL pyramidal cells display correlations between their variabilities (i.e. noise correlations) under stimulation that are strongly time scale and thus frequency dependent (Chacron & Bastian, 2008; Litwin-Kumar *et al.* 2012; Simmonds & Chacron, 2015). Such noise correlations have been shown to strongly impact population coding in other systems (Averbeck & Lee, 2006), and how these mediate population coding in the electrosensory system remains an important and complex problem (Hofmann & Chacron, 2018). Further studies are needed to understand how the activities of ELL pyramidal cells are decoded by downstream brain areas and how processing by these affects behavioural responses.

Function of serotonergic input onto ELL pyramidal cells

Our results have shown that serotonin significantly increased the neural tuning exponent when considering all spikes, although the effect was much greater when considering burst spikes alone. Previous studies have

shown that naturalistic movement envelopes were scale invariant in that spectral power decayed as a power law as a function of increasing temporal frequency up to 1 Hz (Fotowat *et al.* 2013; Metzen & Chacron, 2014). Under control conditions, the neural sensitivity of ELL pyramidal cells increases as a power law with an exponent that is matched to that of the stimulus, such that the resulting response power spectrum is independent of frequency (i.e. temporally whitened), which maximizes information transmission (Huang & Chacron, 2016; Huang *et al.* 2016). However, after serotonin application, the stimulus power spectrum that leads to optimized coding decayed more steeply as characterized by a lower exponent. As such, after serotonin application, the coding of stimuli seen under naturalistic conditions by Metzen and Chacron (2014) is no longer optimized.

To understand these results, it is important to note that the results of Metzen and Chacron (2014) were obtained by averaging over multiple conditions. However, in general, natural stimulus statistics change over multiple time scales and, in order for coding to remain optimized, sensory systems must adapt to such changes (for review see Wark *et al.* 2007; Sharpee *et al.* 2014). As such, it is important to realize that optimized coding for a stimulus with given statistics that occurs under a given context does not imply that coding will be optimized for all stimuli. Indeed, recent studies have shown that the statistics of movement envelopes will change as a function of the animal's environment (Huang *et al.* 2019). Specifically, these are determined from the relative movement between two or more conspecifics; the animal's level of activity will strongly determine how steeply spectral power decays with increasing temporal frequency (i.e. the stimulus exponent). Faster/slower movements thus contribute to increased/decreased high frequency (i.e. around 1 Hz) power, thereby leading to a shallower/steeper decay characterized by a behavioural exponent whose magnitude is smaller/greater. Our results showing an increased neural exponent observed after serotonin application predict that ELL pyramidal neurons will then optimally encode stimuli with greater exponents near −1 (Fig. 6*B*) that are encountered during periods of decreased activity. The steeper decrease in behavioural sensitivity observed after serotonin application provides further support for this hypothesis as this would then lead to a better match between behavioural sensitivity and the statistics of stimuli encountered during periods of decreased activity.

We speculate that the elevated serotonin levels observed in submissive individuals (Larson & Summers, 2001) would not only make these animals move less such as to be less conspicuous and thus not attract the unwanted attention of a dominant individual, but also change neural response properties such as to better detect stimuli associated with them. These include low frequency AMs and electro-communication stimuli but also the movement envelope stimuli considered in this study. As such, our results strongly suggest that an important function of serotonergic feedback is to optimize coding of stimuli encountered by a submissive individual when in the presence of a dominant same-sex individual. Our results are thus consistent with previous ones showing that serotonin acts as a 'shut up and listen' system by inhibiting the display of aggressive behaviours and enhancing the responses of sensory neurons to stimuli associated with dominant same-sex individuals (Maler & Ellis, 1987; Deemyad *et al.* 2013). We also speculate that the enhanced behavioural responses observed here would serve to make the submissive individual appear more dominant and thus potentially ward off further attack. Further studies are, however, needed to verify these predictions.

Implications for other systems

It is likely that our results will be applicable to other systems. This is because optimized coding of natural stimuli through temporal whitening has been observed across systems (visual: Dan *et al.* (1996), Doi *et al.* (2012), Pitkow & Meister (2012); auditory: Rodriguez *et al.* (2010), Theunissen & Elie (2014); somatosensory: Pozzorini *et al.* (2013); vestibular: Mitchell *et al.* (2018)) and, as such, appears to be a universal feature of sensory processing. Together with the fact that the electrosensory system shares many anatomical and functional similarities with other systems (e.g. visual, auditory, vestibular; for review see Clarke *et al.* 2015*a*) supports the hypothesis that our results showing how serotonergic input affects optimized coding of envelopes in the electrosensory system will be applicable to other systems.

Comparative studies have suggested that the serotonergic system is an ancient system that is highly conserved across vertebrate species (Parent, 1981), suggesting a common function. Despite this conservation, studies conducted across systems have revealed multiple functions for serotonergic input. Indeed, while all serotonergic fibres emanate from the raphe nuclei, they make diverse innervation patterns in the brain and act through multiple signalling pathways (Foehring *et al.* 2002; Thompson & Hurley, 2004; Descarries *et al.* 2010), thus leading to a wide range of effects on neuronal activity (Hurley *et al.* 2004; Edeline, 2012). As such, it is likely that our results showing that serotonergic feedback enhances neural and behavioural responses to envelopes associated with same-sex conspecifics will be of interest. We predict that these will be most applicable to other systems for which the distribution and functional role of serotonergic feedback is similar to that observed in the electrosensory system, such as the dorsal cochlear nucleus, which is also a cerebellar-like structure (Felix *et al.* 2017).

Conclusion

We have investigated for the first time the effects of serotonergic input on ELL pyramidal cell and behavioural responses to envelopes in the electrosensory system. Our results show that such input significantly alters neural response properties by promoting burst firing. Our results are, to our knowledge, the first to bring strong evidence that ELL pyramidal cell burst firing is behaviourally relevant. This is because the changes in burst firing observed after serotonin application were the best predictor of changes in behaviour. Moreover, our results show that the mechanisms by which serotonergic feedback alters neural response properties are fundamentally different from those previously uncovered for glutamatergic/GABAergic feedback (Huang *et al.* 2018; Metzen *et al.* 2018). Interestingly, they suggest a novel function for serotonergic feedback in optimizing coding for the statistics of envelope stimuli that a submissive individual would encounter when interacting with dominant same-sex individuals.

References

Averbeck BB & Lee D (2006). Effects of noise correlations on information encoding and decoding. *J Neurophysiol* **95**, 3633–3644.

Avila-Akerberg O, Krahe R & Chacron MJ (2010). Neural heterogeneities and stimulus properties affect burst coding in vivo. *Neuroscience* **168**, 300–313.

Bastian J (1993). The role of amino acid neurotransmitters in the descending control of electroreception. *J Comp Physiol A* **172**, 409–423.

Bastian J, Chacron MJ & Maler L (2002). Receptive field organization determines pyramidal cell stimulus-encoding capability and spatial stimulus selectivity. *J Neurosci* **22**, 4577–4590.

Bell C & Maler L (2005). Central neuroanatomy of electrosensory systems in fish. In *Electroreception*, ed. Bullock TH, Hopkins CD, Popper AN & Fay RR, pp. 68–111. Springer, New York.

Berman NJ & Maler L (1999). Neural architecture of the electrosensory lateral line lobe: adaptations for coincidence detection, a sensory searchlight and frequency-dependent adaptive filtering. *J Exp Biol* **202**, 1243–1253.

Chacron MJ & Bastian J (2008). Population coding by electrosensory neurons. *J Neurophysiol* **99**, 1825–1835.

Chacron MJ, Longtin A & Maler L (2011). Efficient computation via sparse coding in electrosensory neural networks. *Curr Opin Neurobiol* **21**, 752–760.

Clarke SE, Longtin A & Maler L (2015*a*). Contrast coding in the electrosensory system: parallels with visual computation. *Nat Rev Neurosci* **16**, 733–744.

Clarke SE, Longtin A & Maler L (2015*b*). The neural dynamics of sensory focus. *Nat Commun* **6**, 8764.

Dan Y, Atick JJ & Reid RC (1996). Efficient coding of natural scenes in the lateral geniculate nucleus: experimental test of a computational theory. *J Neurosci* **16**, 3351–3362.

Deemyad T, Maler L & Chacron MJ (2011). Inhibition of SK and M channel-mediated currents by 5-HT enables parallel processing by bursts and isolated spikes. *J Neurophysiol* **105**, 1276–1294.

Deemyad T, Metzen MG, Pan Y & Chacron MJ (2013). Serotonin selectively enhances perception and sensory neural responses to stimuli generated by same-sex conspecifics. *Proc Natl Acad Sci U S A* **110**, 19609–19614.

Descarries L, Riad M & Parent M (2010). Ultrastructure of the serotonin innervation in mammalian CNS. In *Handbook of the Behavioural Neurobiology of Serotonin*, ed. Muller CP & Jacobs BL, pp 65–101. Academic Press, London, UK.

Doi E, Gauthier JL, Field GD, Shlens J, Sher A, Greschner M, Machado TA, Jepson LH, Mathieson K, Gunning DE, Litke AM, Paninski L, Chichilnisky EJ & Simoncelli EP (2012). Efficient coding of spatial information in the primate retina. *J Neurosci* **32**, 16256–16264.

Edeline JM (2012). Beyond traditional approaches to understanding the functional role of neuromodulators in sensory cortices. *Front Behav Neurosci* **6**, 45.

Ellis LD, Mehaffey WH, Harvey-Girard E, Turner RW, Maler L & Dunn RJ (2007). SK channels provide a novel mechanism for the control of frequency tuning in electrosensory neurons. *J Neurosci* **27**, 9491–9502.

Felix RA 2nd, Elde CJ, Nevue AA & Portfors CV (2017). Serotonin modulates response properties of neurons in the dorsal cochlear nucleus of the mouse. *Hear Res* **344**, 13–23.

Foehring RC, van Brederode JF, Kinney GA & Spain WJ (2002). Serotonergic modulation of supragranular neurons in rat sensorimotor cortex. *J Neurosci* **22**, 8238–8250.

Fotowat H, Harrison RR & Krahe R (2013). Statistics of the electrosensory input in the freely swimming weakly electric fish Apteronotus leptorhynchus. *J Neurosci* **33**, 13758–13772.

Frank K & Becker MC (1964). Microelectrodes for recording and stimulation. In *Physical Techniques in Biological Research*, ed. Nastuk WL, pp. 23–84. Academic Press, New York.

Gabbiani F, Metzner W, Wessel R & Koch C (1996). From stimulus encoding to feature extraction in weakly electric fish. *Nature* **384**, 564–567.

Heiligenberg W (1991). *Neural Nets in Electric Fish*. MIT Press, Cambridge MA.

Hitschfeld EM, Stamper SA, Vonderschen K, Fortune ES & Chacron MJ (2009). Effects of restraint and immobilization on electrosensory behaviors of weakly electric fish. *ILAR J* **50**, 361–372.

Hofmann V & Chacron MJ (2018). Population coding and correlated variability in electrosensory pathways. *Front Integr Neurosci* **12**, 56.

Huang CG & Chacron MJ (2016). Optimized parallel coding of second-order stimulus features by heterogeneous neural populations. *J Neurosci* **36**, 9859–9872.

Huang CG & Chacron MJ (2017). SK channel subtypes enable parallel optimized coding of behaviorally relevant stimulus attributes: A review. *Channels* **11**, 281–304.

Huang CG, Metzen MG & Chacron MJ (2018). Feedback optimizes neural coding and perception of natural stimuli. *Elife* **7**, e38935.

Huang CG, Metzen MG & Chacron MJ (2019). Descending pathways mediate adaptive optimized coding of natural stimuli in weakly electric fish. *Sci Adv* **5**, eaax2211.

Huang CG, Zhang ZD & Chacron MJ (2016). Temporal decorrelation by SK channels enables efficient neural coding and perception of natural stimuli. *Nat Commun* **7**, 11353.

Hupe GJ & Lewis JE (2008). Electrocommunication signals in free swimming brown ghost knifefish, *Apteronotus leptorhynchus*. *J Exp Biol* **211**, 1657–1667.

Hurley LM, Devilbiss DM & Waterhouse BD (2004). A matter of focus: monoaminergic modulation of stimulus coding in mammalian sensory networks. *Curr Opin Neurobiol* **14**, 488–495.

Johnston SA, Maler L & Tinner B (1990). The distribution of serotonin in the brain of *Apteronotus leptorhynchus*: an immunohistochemical study. *J Chem Neuroanat* **3**, 429–465.

Kepecs A & Lisman J (2003). Information encoding and computation with spikes and bursts. *Network* **14**, 103–118.

Khosravi-Hashemi N & Chacron MJ (2012). Bursts and isolated spikes code for opposite movement directions in midbrain electrosensory neurons. *PLoS One* **7**, e40339.

Khosravi-Hashemi N & Chacron MJ (2014). Motion processing across multiple topographic maps in the electrosensory system. *Physiol Rep* **2**, e00253.

Khosravi-Hashemi N, Fortune ES & Chacron MJ (2011). Coding movement direction by burst firing in electrosensory neurons. *J Neurophysiol* **106**, 1954–1968.

Krahe R & Gabbiani F (2004). Burst firing in sensory systems. *Nat Rev Neurosci* **5**, 13–23.

Krahe R & Maler L (2014). Neural maps in the electrosensory system of weakly electric fish. *Curr Opin Neurobiol* **24**, 13–21.

Larson EA, Metzen MG & Chacron MJ (2014). Serotonin modulates electrosensory processing and behavior via 5-HT2-like receptors. *Neuroscience* **271**, 108–118.

Larson ET & Summers CH (2001). Serotonin reverses dominant social status. *Behav Brain Res* **121**, 95–102.

Lemon N & Turner RW (2000). Conditional spike backpropagation generates burst discharge in a sensory neuron. *J Neurophysiol* **84**, 1519–1530.

Lisman JE (1997). Bursts as a unit of neural information: making unreliable synapses reliable. *Trends Neurosci* **20**, 38–43.

Litwin-Kumar A, Chacron MJ & Doiron B (2012). The spatial structure of stimuli shapes the timescale of correlations in population spiking activity. *PLoS Comput Biol* **8**, e1002667.

Maler L & Ellis WG (1987). Inter-male aggressive signals in weakly electric fish are modulated by monoamines. *Behav Brain Res* **25**, 75–81.

Marder E (2012). Neuromodulation of neuronal circuits: back to the future. *Neuron* **76**, 1–11.

Marquez BT, Krahe R & Chacron MJ (2013). Neuromodulation of early electrosensory processing in gymnotiform weakly electric fish. *J Exp Biol* **216**, 2442–2450.

Marquez MM & Chacron MJ (2018). Serotonin selectively increases detectability of motion stimuli in the electrosensory system. *eNeuro* **5**, ENEURO.0013-0018.2018.

Marsat G, Longtin A & Maler L (2012). Cellular and circuit properties supporting different sensory coding strategies in electric fish and other systems. *Curr Opin Neurobiol* **22**, 686–692.

Marsat G & Maler L (2012). Preparing for the unpredictable: adaptive feedback enhances the response to unexpected communication signals. *J Neurophysiol* **107**, 1241–1246.

Marsat G & Pollack GS (2006). A behavioral role for feature detection by sensory bursts. *J Neurosci* **26**, 10542–10547.

McMillan GA & Gray JR (2015). Burst firing in a motion-sensitive neural pathway correlates with expansion properties of looming objects that evoke avoidance behaviors. *Front Integr Neurosci* **9**, 60.

Metzen MG & Chacron MJ (2014). Weakly electric fish display behavioral responses to envelopes naturally occurring during movement: implications for neural processing. *J Exp Biol* **217**, 1381–1391.

Metzen MG & Chacron MJ (2019). Envelope coding and processing: implications for perception and behavior. In *Electroreception: Fundamental Insights from Comparative Approaches*, ed. Carlson B, Sisneros J, Popper A & Fay R, pp. 251–277. Springer, Cham.

Metzen MG, Huang CG & Chacron MJ (2018). Descending pathways generate perception of and neural responses to weak sensory input. *PLoS Biol* **16**, e2005239.

Mitchell DE, Kwan A, Carriot J, Chacron MJ & Cullen KE (2018). Neuronal variability and tuning are balanced to optimize naturalistic self-motion coding in primate vestibular pathways. *Elife* **7**, e43019.

Noonan L, Doiron B, Laing C, Longtin A & Turner RW (2003). A dynamic dendritic refractory period regulates burst discharge in the electrosensory lobe of weakly electric fish. *J Neurosci* **23**, 1524–1534.

Oswald AMM, Chacron MJ, Doiron B, Bastian J & Maler L (2004). Parallel processing of sensory input by bursts and isolated spikes. *J Neurosci* **24**, 4351–4362.

Parent A (1981). Comparative anatomy of the serotoninergic systems. *J Physiol (Paris)* **77**, 147–156.

Pitkow X & Meister M (2012). Decorrelation and efficient coding by retinal ganglion cells. *Nat Neurosci* **15**, 628–635.

Pozzorini C, Naud R, Mensi S & Gerstner W (2013). Temporal whitening by power-law adaptation in neocortical neurons. *Nat Neurosci* **16**, 942–948.

Rieke F, Warland D, de Ruyter van Steveninck RR & Bialek W (1996). *Spikes: Exploring the Neural Code*. MIT, Cambridge, MA.

Risken H (1996). *The Fokker-Planck Equation*. Springer, Berlin.

Rodriguez FA, Chen C, Read HL & Escabi MA (2010). Neural modulation tuning characteristics scale to efficiently encode natural sound statistics. *J Neurosci* **30**, 15969–15980.

Sas E & Maler L (1983). The nucleus praeeminentialis: A Golgi study of a feedback center in the electrosensory system of gymnotid fish. *J Comp Neurol* **221**, 127–144.

Sas E & Maler L (1987). The organization of afferent input to the caudal lobe of the cerebellum of the gymnotid fish *Apteronotus leptorhynchus*. *Anat Embryol* **177**, 55–79.

Sharpee TO, Calhoun AJ & Chalasani SH (2014). Information theory of adaptation in neurons, behavior, and mood. *Curr Opin Neurobiol* **25**, 47–53.

Simmonds B & Chacron MJ (2015). Activation of parallel fiber feedback by spatially diffuse stimuli simultaneously reduces signal and noise correlations via independent mechanisms in a cerebellum-like structure. *PLoS Comp Biol* **11**, e1004034.

Theunissen FE & Elie JE (2014). Neural processing of natural sounds. *Nat Rev Neurosci* **15**, 355–366.

Thompson AM & Hurley LM (2004). Dense serotonergic innervation of principal nuclei of the superior olivary complex in mouse. *Neurosci Lett* **356**, 179–182.

Toporikova N & Chacron MJ (2009). Dendritic SK channels gate information processing *in vivo* by regulating an intrinsic bursting mechanism seen *in vitro*. *J Neurophysiol* **102**, 2273–2287.

Turner RW, Maler L & Burrows M (1999). Electroreception and electrocommunication. *J Exp Biol* **202**, 1167–1458.

Wark B, Lundstrom BN & Fairhall A (2007). Sensory adaptation. *Curr Opin Neurobiol* **17**, 423–429.

Yu N, Hupe G, Garfinkle C, Lewis JE & Longtin A (2012). Coding conspecific identity and motion in the electric sense. *PLoS Comput Biol* **8**, e1002564.

Additional information

Competing interests

The authors declare no conflict of interest.

Author contributions

M.J.C. designed research, M.M.M. performed research, M.M.M. and M.J.C. wrote and revised the manuscript. Both authors approved the final version of the manuscript and agree to be accountable for all aspects of the work in ensuring that questions related to the accuracy or integrity of any part of the work are appropriately investigated and resolved. All persons designated as authors qualify for authorship, and all those who qualify for authorship are listed.

Funding

Keywords

Supporting information

Additional supporting information may be found online in the Supporting Information section at the end of the article.

Statistical Summary Document.